Strasbourg (France)

MANUSCRIPT COVER PAGE FORM

E-MRS Symposium : D

Paper number : #2040

Title of paper : ION-IMPLANT SIMULATIONS: THE EFFECT OF DEFECT SPATIAL CORRELATION ON DAMAGE ACCUMULATION.

Corresponding author : K. R. C. Mok

Full Mailing Address : Caroline Mok. Dpto. Electronica. Universidad de Valladolid. E.T.S.I.T. Campus Miguel Delibes S/N. 47011. Valladolid. Spain.

Telephone : +34 983 42 30 00 ext 5510

Fax : +34 983 42 36 75

E-mail : g0202446@nus.edu.sg

Ion-implant simulations: The effect of defect spatial correlation on damage accumulation

K. R. C. Mok,[1,2] M. Jaraiz,[1] I. Martin-Bragado,[1,3] J. E. Rubio,[1]
P. Castrillo,[1] R. Pinacho,[1] M. P. Srinivasan,[2] and F. Benistant[4]

[1]*Departamento de E. y Electrónica,*
Universidad de Valladolid. ETSIT Campus Miguel Delibes, 47011 Valladolid, Spain

[2]*Department of Chemical & Biomolecular Engineering,*
National University of Singapore. 4 Engineering Drive 4, Singapore 117576

[3]*Synopsys. Karl-Hammerschmidt Strasse 34,*
D-85609 Aschheim/Dornach, Germany

[4]*Chartered Semiconductor Manufacturing. 60 Woodlands*
Industrial Park D, Street 2, Singapore 738406.

Abstract

A predictive damage accumulation model, which takes into account different interdependent implant parameters, has been developed. The model assumes that the recrystallization rate of damage structures known as amorphous pockets (AP) is a function of its effective size, regardless of their spatial configuration. In the model, APs are three-dimensional agglomerates of interstitials (I) and vacancies (V), whose initial coordinates are generated by a binary collision approximation (BCA) code. This work addresses the importance of the spatial correlation of I's and V's in modeling damage accumulation and amorphization, by comparing simulations whereby the initial coordinates of I and V are generated by BCA or randomly generated from the concentration distribution of an input damage profile. Low temperature implantations were simulated to avoid dynamic annealing in order to compare the initial damage morphology. For the same damage level, simulations by BCA resulted in ion mass dependent APs' sizes, with lighter implant ions generating smaller APs' sizes, implying more dilute damage compared with heavier ions. However, the ion mass dependent APs' size effect was lost by loading the same damage profile and randomly positioning the I's and V's. Consequently, the damage morphology, as well as the annealing behaviour obtained by reading I, V damage profiles is substantially different from those obtained using the much more realistic cascades generated by BCA.

I. INTRODUCTION

Ion-implant processing is a field of considerable scientific and technological interest, as it is a standard process in introducing dopants in integrated circuit (IC) devices. Modeling and prediction of ion-implant induced damage accumulation is crucial to the simulation of silicon processing. A single accurate model should account for experimental observations, taking into account ion mass, dose, dose rate and substrate temperature effects. In addition, the model should be implemented in a manner efficient for practical device-sized process simulations.

In process simulators, implant damage distribution in terms of interstitials (I) and vacancies (V) is commonly generated by means of an analytical approximation or a binary collision approximation (BCA) code. It has been shown [1] using an atomistic non-lattice kinetic Monte Carlo (kMC) [2], that the spatial correlation of the (I,V) Frenkel pairs is not critical for modeling transient enhanced diffusion (TED) in cases without immobile impurity-point defect clusters. Whether the initial coordinates of the particles are provided by a BCA simulator or randomly generated following the concentration distribution of an input profile, TED simulation results are similar. This work looks at whether the same is true for damage accumulation and amorphization.

II. OUR MODEL

We have developed a model, based on damage structures known as amorphous pockets (AP, [3]), that accounts for the many interdependent implantation parameters. In this model, the coordinates of the ion-implantation induced Frenkel pairs obtained from the binary collision (BCA) program [4] are inserted, cascade after cascade, into an atomistic non-lattice kinetic Monte Carlo simulator [2]. Instead of undergoing immediate recrystallization, I's and V's form a distinct, disordered region (I_nV_m) when they are within a capture distance (second neighbor distance) of each other. The AP recrystallization rate (shrinkage rate) is characterized by the effective size of the AP (s=min(n, m)), and the activation energy for recrystallization is assumed to be a function of this number alone, irrespective of its internal spatial configuration.

In process simulations, damage can be obtained from BCA, preserving the I, V spatial

correlation, or it can be randomly generated from an input I, V concentration profile. Although the internal spatial configuration of the APs is not important in this model, we will test if the spatial correlation of I, V is critical in modeling damage accumulation. Implant simulations were done using damage generated by binary collision or by using I, V concentration profiles as inputs. Since the concentration profiles are translated into particle coordinates using a random number generator, all I, V spatial correlation is lost. The implant simulations were done at low temperature (100 K) to avoid dynamic annealing or defect migration, in order to compare their initial damage morphology.

III. SIMULATION RESULTS

Figure 1 shows the AP histograms resulting from BCA implants of C and Xe at different damage concentrations. Implantation parameters were varied so as to achieve a relatively constant damage concentration across the simulated depth. As heavier implant ions generate more damage for the same implant energy, a smaller dose of Xe compared to C is required to achieve the same level of damage.

The same level of damage is attained by APs of different sizes depending on the implant ion. C (12 amu) being a lighter implant ion, generates APs of smaller sizes compared to Xe (132 amu). At all damage levels, the AP size distribution obtained from the heavier implant ion is broader. The shapes of the AP histograms for both implant ions are similar at low damage concentrations. The concentration of APs increases proportionally with increasing damage concentration, indicating isolated collision cascades. For C at damage concentrations of $1 \times 10^{20}\,\mathrm{cm}^{-3}$ and above, the AP histograms have higher proportion of larger sized APs, implying overlapping cascades. For Xe, (Fig. 2) the overlapping of collision cascades becomes only evident at a higher concentration of $1 \times 10^{21}\,\mathrm{cm}^{-3}$, due to the denser collision cascades induced by the heavier ion.

The difference in size distribution of the APs generated by C and Xe BCA implants at the same damage concentration of $1 \times 10^{20}\,\mathrm{cm}^{-3}$ can be more clearly seen from the 2D color maps shown in Fig. 3. Notice the small but distinct net balance towards the V axis, indicating a deficit of atoms (nI<mV) in the APs, in agreement with MD study [5], despite the fact that a binary collision program has been used for the development of the collisional phase of the cascades in our case. Not shown in the color map is the presence of a higher amount of

isolated interstitial point defects compared to vacancy point defects, also in agreement with Ref. [5].

The dependence of the size of APs with ion mass allows for the modeling of dynamic annealing, which accounts for ion mass effects. MD simulations [3] have shown that larger APs are more stable as evidenced by their higher apparent activation energy for recrystallization. Taking the activation energy for recrystallization to be size-dependent, whereby the activation energy increases with the size of APs, a higher implant temperature will be required to dynamically anneal larger defects. As APs generated by heavier implant ions are extended towards larger sizes, this enables the modeling of the amorphous-crystalline transition temperature, which increases with ion mass [6].

Instead of performing a BCA implant, the I's and V's can be generated by reading an existing damage concentration profile. Without using the BCA code to directly generate the implant cascades, the defect particle coordinates were obtained from the concentration profile randomly, thereby losing all the I, V spatial correlation.

Figure 4 shows the AP histograms resulting from BCA implants of H, C and Xe and by reading damage profiles of C and Xe. In all cases, the total damage concentration is about $1 \times 10^{20}\,\mathrm{cm}^{-3}$. Using BCA implants, the AP size dependence on implant ion mass is clearly evident. By reading damage profiles, the ion mass effect on APs is lost and the concentration of APs is much lower compared to those obtained from BCA (the damage missing in the histograms is in the form of isolated I's and V's). Furthermore, they are concentrated at very small sizes, even smaller than those APs generated by a BCA implant of a very light implant ion, like H. As the I, V coordinates are randomly generated by reading damage profiles, the I, V defects are more likely to be point defects instead of being close enough to form APs.

With this model, using the BCA implant and calibrating the activation energy for recrystallization, the amorphous-crystalline transition temperature for C, Si and Ge can be accurately reproduced based on Ref. [6], whereby 80 keV implant at various dose rates were done up to a dose of $1 \times 10^{15}\,\mathrm{cm}^{-2}$ for Si and Ge, and $2 \times 10^{15}\,\mathrm{cm}^{-2}$ for C. At a dose rate of $5 \times 10^{12}\,\mathrm{cm}^{-2}\mathrm{s}^{-1}$, the amorphous-crystalline transition temperatures for C, Si and Ge are 20 °C, 75 °C and 165 °C respectively. Instead, reading damage profiles of these simulations, the amorphous-crystalline temperature obtained for C is 20 °C, 35 °C for Si and 60 °C for Ge. Therefore, the damage morphology, as well as the annealing behaviour obtained by

reading I, V damage profiles is substantially different from those obtained using the much more realistic cascades generated by BCA.

IV. CONCLUSIONS

In summary, I, V spatial correlation is important in order to take into account ion mass effects. Even though the AP recombination rate is only size dependent and does not take into account internal spatial configuration of the AP, the I, V spatial correlation is important in order to form the initial APs with a size distribution dependent on ion mass. For the same damage level, simulations by BCA, which preserves the I, V spatial correlation, resulted in AP sizes with ion mass dependence, with lighter implant ions generating more dilute damage. This ion mass dependent APs' size effect was lost by reading the same damage profile and randomly positioning the I's and V's. Therefore, in order to model damage accumulation taking into account the ion mass effect, it is essential to keep the spatial correlation of the I's and V's in the collision cascades as generated by BCA (or by MD).

List of References

---

[1] I. Martin-Bragado, M. Jaraiz, P. Castrillo, R. Pinacho, J. E. Rubio, and J. Barbolla, Appl. Phys. Lett. **84**, 4962 (2004).

[2] M. Jaraiz, P. Castrillo, R. Pinacho, I. Martin-Bragado, and J. Barbolla, in *Simulation of Semiconductor Processes and Devices 2001*, edited by D. Tsoukalas and C. Tsamis (Springer-Verlag, Vienna, 2001), pp. 10–17.

[3] M. J. Caturla, T. Diaz de la Rubia, L. A. Marques, and G. H. Gilmer, Phys. Rev. B **54**, 16683 (1996).

[4] M. T. Robinson, Phys. Rev. B **40**, 10717 (1989).

[5] K. Nordlund, M. Ghaly, R. S. Averback, M. Caturla, T. Diaz de la Rubia, and J. Tarus, Phys. Rev. B **57**, 7556 (1998).

[6] R. D. Goldberg, J. S. Williams, and R. G. Elliman, Nucl. Instrum. Meth. B **106**, 242 (1995).

List of figure captions

FIG 1. AP histograms obtained from C (lines with symbols) and Xe (dotted lines) implants using BCA at different damage concentrations.

FIG 2. Normalized AP distribution obtained from Xe implants using BCA at different damage concentrations.

FIG 3. 2D color maps showing the AP size distribution at a constant damage of $1 \times 10^{20}\,\mathrm{cm}^{-3}$ generated by BCA implant of (a) C and (b) Xe.

FIG 4. AP histograms at a constant damage concentration of $1 \times 10^{20}\,\mathrm{cm}^{-3}$, of BCA H, C and Xe implants and by loading damage profiles of C and Xe.

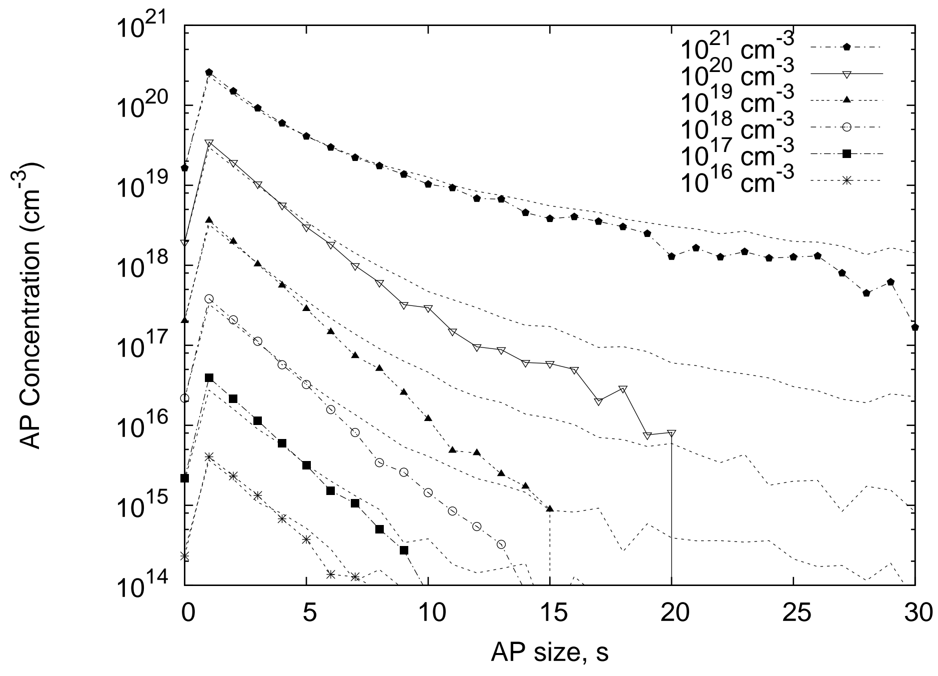

FIG. 1:

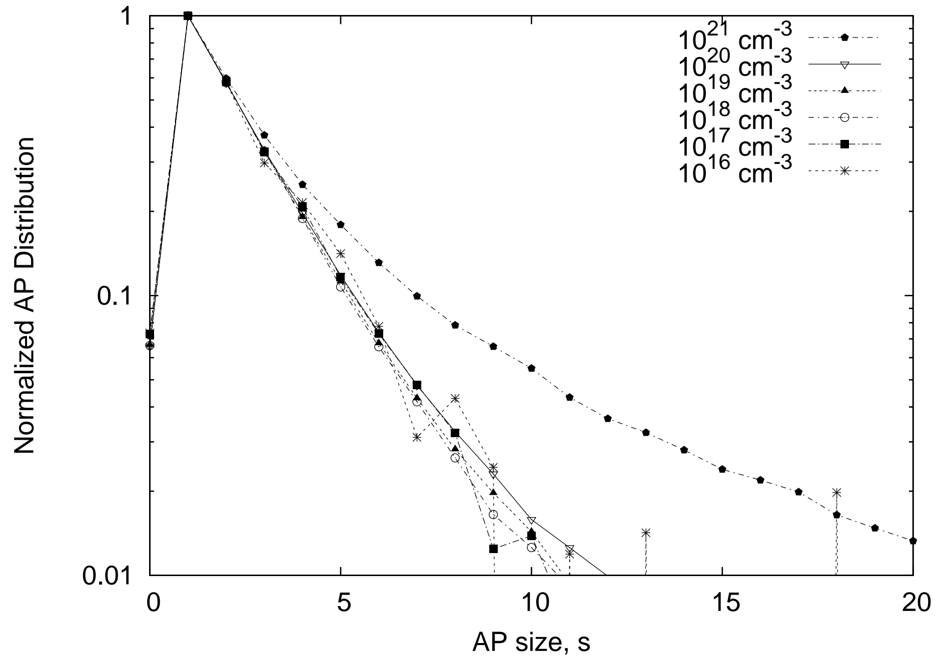

FIG. 2:

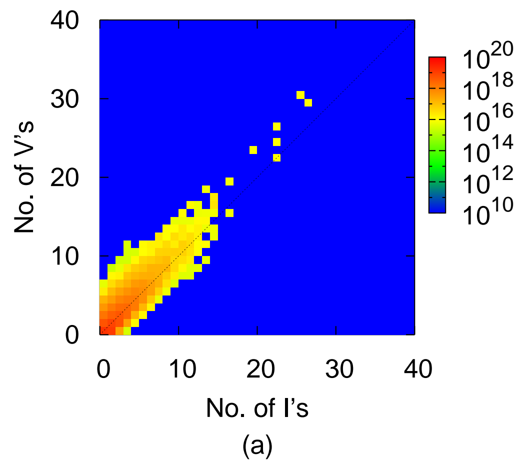

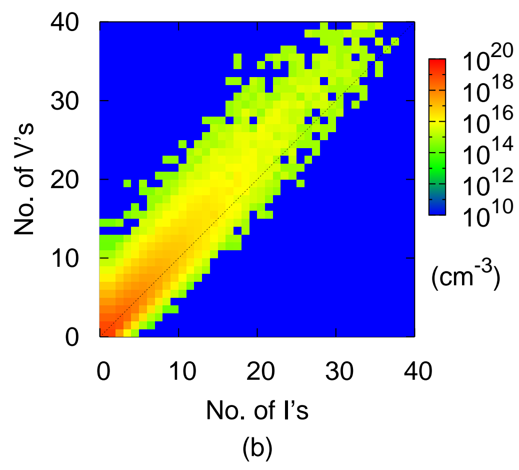

FIG. 3:

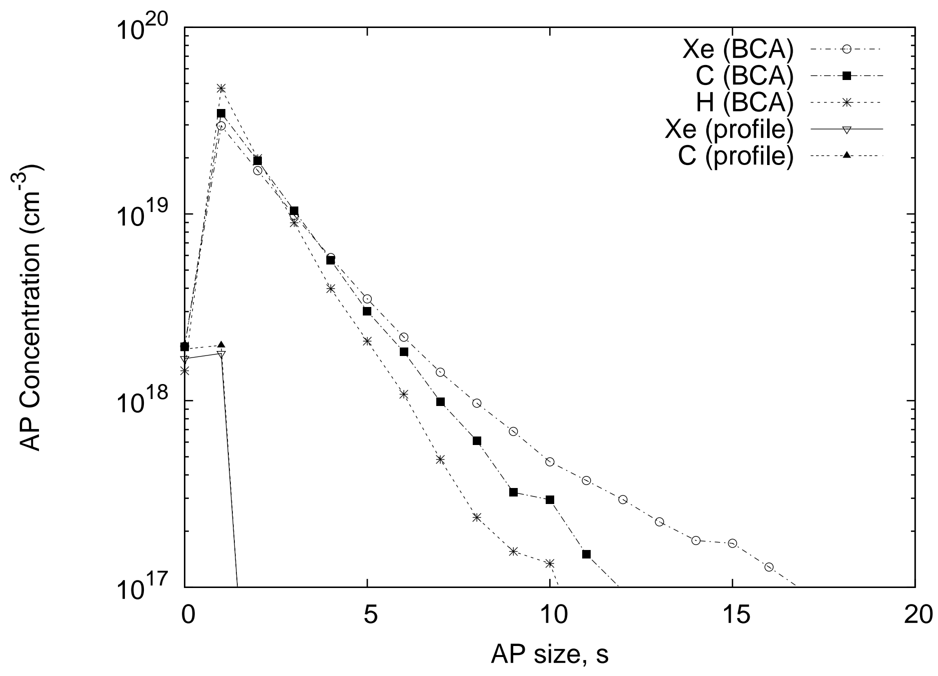

FIG. 4: